ACCOUNTS of chemical research

Article

pubs.acs.org/accounts

Atomic Layer Deposition of Metal Sulfide Materials

Neil P. Dasgupta,*[,†,∥] Xiangbo Meng,[‡,∥] Jeffrey W. Elam,*[,‡] and Alex B. F. Martinson*[,§]

[†]Department of Mechanical Engineering, University of Michigan, Ann Arbor, Michigan 41809, United States

[‡]Energy Systems Division, Argonne National Laboratory, Argonne, Illinois 60439, United States

[§]Materials Science Division, Argonne National Laboratory, Argonne, Illinois 60439, United States

CONSPECTUS: The field of nanoscience is delivering increasingly intricate yet elegant geometric structures incorporating an ever-expanding palette of materials. Atomic layer deposition (ALD) is a powerful driver of this field, providing exceptionally conformal coatings spanning the periodic table and atomic-scale precision independent of substrate geometry. This versatility is intrinsic to ALD and results from sequential and self-limiting surface reactions. This characteristic facilitates digital synthesis, in which the film grows linearly with the number of reaction cycles. While the majority of ALD processes identified to date produce metal oxides, novel applications in areas such as energy storage, catalysis, and nanophotonics are motivating interest in sulfide materials. Recent progress in ALD of sulfides has expanded the diversity of accessible materials as well as a more complete understanding of the unique chalcogenide surface chemistry.

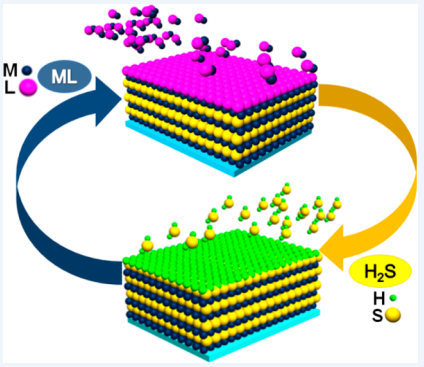

ALD of sulfide materials typically uses metalorganic precursors and hydrogen sulfide (H_2S). As in oxide ALD, the precursor chemistry is critical to controlling both the film growth and properties including roughness, crystallinity, and impurity levels. By modification of the precursor sequence, multicomponent sulfides have been deposited, although challenges remain because of the higher propensity for cation exchange reactions, greater diffusion rates, and unintentional annealing of this more labile class of materials. A deeper understanding of these surface chemical reactions has been achieved through a combination of in situ studies and quantum-chemical calculations. As this understanding matures, so does our ability to deterministically tailor film properties to new applications and more sophisticated devices.

This Account highlights the attributes of ALD chemistry that are unique to metal sulfides and surveys recent applications of these materials in photovoltaics, energy storage, and photonics. Within each application space, the benefits and challenges of novel ALD processes are emphasized and common trends are summarized. We conclude with a perspective on potential future directions for metal chalcogenide ALD as well as untapped opportunities. Finally, we consider challenges that must be addressed prior to implementing ALD metal sulfides into future device architectures.

INTRODUCTION

Atomic layer deposition (ALD) is a powerful technique that is capable of depositing a wide range of materials with subnanometer precision.[1] It is a modified version of chemical vapor deposition (CVD), in which gas-phase precursors are exposed to a substrate in a sequential manner, separated by inert-gas purging. A critical requirement for ALD is self-limiting surface chemistry, such that each precursor reacts selectively with surface functional groups and does not thermally decompose. After saturation of the first species, the remaining molecules are purged away, and a second self-limiting precursor is introduced. Repeating these sequential exposures results in constant material growth per cycle (GPC). This provides conformal coating of ultrahigh-aspect-ratio structures (>2000:1) without gradients in thickness or composition. A schematic illustration of the binary ALD process is shown in Scheme 1.

ALD has been explored for a wide range of applications, most notably in the semiconductor industry. The majority of ALD materials that have been deposited are metal oxides because of the commercial demand for thin-film dielectrics. These can be either binary oxides or multicomponent alloys depending on the sequence of precursor sources utilized.

Recently, interest in ALD of sulfide materials has increased, driven partially by energy and photonic applications. For example, earth-abundant sulfide materials are of interest in solar cell applications as potential low-cost alternatives to silicon. Transition-metal sulfides have also emerged as attractive catalysts. In addition, metal sulfides are promising electrodes and electrolytes for electrical energy storage applications, such as lithium−sulfur (Li−S) batteries. The advantages of ALD, including precise thickness and compositional control as well as conformal coating of complex geometries, make it attractive for surface and interfacial engineering of these devices.

While some of the earliest ALD processes used elemental sulfur as the anion source,[2] the vast majority of ALD sulfide processes use H_2S because of its greater volatility and reactivity with metalorganic precursors. Despite these advantages, H_2S presents several challenges for incorporation in ALD. In particular, H_2S is a flammable, corrosive, and toxic gas, and

Received: October 15, 2014
Published: January 12, 2015

DOI: 10.1021/ar500360d
Acc. Chem. Res. 2015, 48, 341−348

Scheme 1. Illustration of the ALD Process

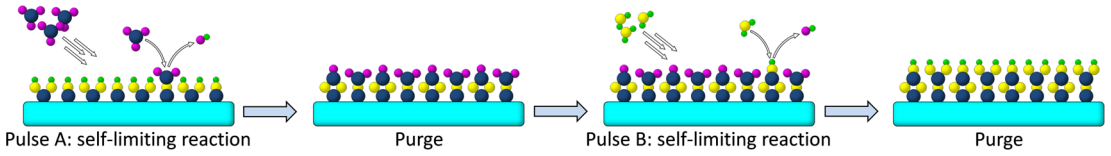

these properties demand careful consideration when designing an ALD reactor for H_2S compatibility, as described in detail elsewhere.[3]

With H_2S, a variety of sulfide materials may be deposited by ALD, and the list is rapidly expanding. In this Account, we summarize recent work on sulfide ALD, with an emphasis on energy and photonic applications. This is not intended to be a comprehensive review, but rather a highlight of the range of sulfide materials that can be deposited and an illustration of the advantages and limitations of ALD in this application space.

PREVIOUS WORK

Early ALD experiments in the 1970s examined ZnS for thin film electroluminescent (TFEL) displays.[2,4] However, in contrast to the vast literature on oxide ALD, only 16 binary sulfides have been studied to date, including ZnS (1977),[5] CaS (1987),[6] BaS (1987),[6] SrS (1987),[6] CdS (1988),[7] PbS (1990),[8] In_2S_3 (1994),[9] Cu_xS (2001),[10] WS_2 (2004),[11] TiS_2 (2007),[12] Sb_2S_3 (2009),[13] SnS (2010),[14] GaS_x (2013),[15,16] GeS (2014),[17] MoS_2 (2014),[18] and Li_2S (2014)[19] in chronological order. By combining two or more binary sulfide processes, ALD can also produce complex multicomponent sulfides.[20,21]

The precursors play a critical role in ALD, as their chemistry governs the growth and properties of the deposited films. Ideally, ALD precursors should be volatile, thermally stable, and highly reactive toward the coreactant. The earliest experiments utilized elemental Zn and S for ZnS ALD at ∼500 °C, and the self-limiting growth depended on the slightly higher binding energy for the first monolayer compared with subsequent layers.[2,5] Shortly thereafter, atomic precursors were mostly abandoned in favor of molecular precursors, such as $ZnCl_2$ (and later ZnI_2[22]) and H_2S,[2,4] where ligand-exchange reactions provide more reliable self-limitation. However, halide precursors often require high source temperatures of 300−400 °C for vaporization, necessitating equal or greater deposition temperatures, which poses challenges for some applications. Additionally, halide impurities are deleterious in many applications.

In view of these shortcomings, numerous metalorganic precursors have been investigated, many of which have yielded superior processes. For further details, readers may refer to Puurunen's publications.[23,24] In each case, H_2S was used exclusively as the S source. Among the metalorganics, the alkyls ($ZnMe_2$, $ZnEt_2$, and $CdMe_2$) have enabled the largest temperature range and highest GPCs because of their high reactivity and thermal stability. When $ZnEt_2$ and H_2S are used, the ZnS GPC decreases monotonically with increasing temperature.[25] This has been observed in all of the ALD processes using alkyls and H_2S.[25−27] Similar trends have been observed in several other ALD processes with H_2S and are commonly attributed to a decrease in surface functional group coverage with increasing temperature. In contrast, increasing GPCs with temperature were reported for some β-diketonate precursors, including $Ba(thd)_2$ (thd = 2,2,6,6-tetramethyl-3,5-heptanedionate).[28] Temperature-independent growth with H_2S has also been observed in some studies, including with $Li(O^tBu)$[19] and $Sn(^iPrAMD)_2$ (^iPrAMD = *N*,*N*′-diisopropylacetamidinato).[29]

The growth temperature can also affect the film roughness, crystallinity, and composition. For instance, pure crystalline CuS was formed at temperatures below 175 °C using $Cu(thd)_2$, while pure crystalline $Cu_{1.8}S$ was deposited at higher temperatures.[10] Similarly, $Sn(NMe_2)_3$ produced amorphous SnS_2 below 120 °C, hexagonal SnS_2 at 140−150 °C, and orthorhombic SnS above 160 °C.[30] In both cases, the roughness increased with temperature. However, it was reported recently that only amorphous phases were produced in ALD of both GaS_x and Li_2S,[15,19] and the resulting films had comparable roughness over the entire temperature range. Thus, there are no well-established rules to date to predict the growth and properties of ALD sulfide films. Variations in growth characteristics are likely dictated by the properties of individual precursors, and future studies should lead to novel insights and greater predictive capacity for sulfide ALD.

SURFACE CHEMISTRY OF SULFIDE ALD

A detailed understanding of the surface chemical processes that govern ALD can be invaluable for precursor design, process selection, and even ALD reactor engineering. While there have been relatively few surface chemical studies of sulfide ALD, the processes investigated to date follow a ligand-exchange mechanism in which surface thiols (−SH) play the same role as surface hydroxyls (−OH) in oxide ALD. The overall reaction can be written as $ML_x + (x/2)H_2S \rightarrow MS_{x/2} + xHL$, where ML_x is the precursor of metal M with x ligands L. The self-limiting characteristic of ALD greatly simplifies in situ mechanistic studies, since the surface remains "frozen" after each precursor exposure, allowing the surface species to be examined in detail. As a case study, we consider Ga_2S_3 ALD using alternating exposures of $Ga(N(CH_3)_2)_3$ and H_2S.[15] In situ Fourier transform infrared (FTIR) absorption measurements revealed the exchange of surface SH groups for $N(Me)_2$ groups during each $Ga(N(CH_3)_2)_3$ exposure and vice versa during the subsequent H_2S precursor exposure (Figure 1a). Moreover, in situ quadrupole mass spectrometry (QMS) measurements established that dimethylamine (DMA) is the only gas-phase product released. Therefore, we can postulate a set of ALD surface reactions:

$$|{-}(SH)_x + Ga(N(CH_3)_2)_3(g) \rightarrow |{-}S_x{-}Ga(N(CH_3)_2)_{(3-x)} + xHN(CH_3)_2(g) \quad (1)$$

$$|{-}S_x{-}Ga(N(CH_3)_2)_{(3-x)} + 1.5H_2S(g) \rightarrow |{-}(GaS_{1.5}){-}(SH)_x + (3-x)HN(CH_3)_2(g) \quad (2)$$

where "|−" represents the surface. The stoichiometry of these reactions (i.e., the value of x) can be determined in one of two ways: by measuring the relative amount of DMA produced in each half-reaction via QMS or by measuring the fraction of

DOI: 10.1021/ar500360d
Acc. Chem. Res. 2015, 48, 341−348

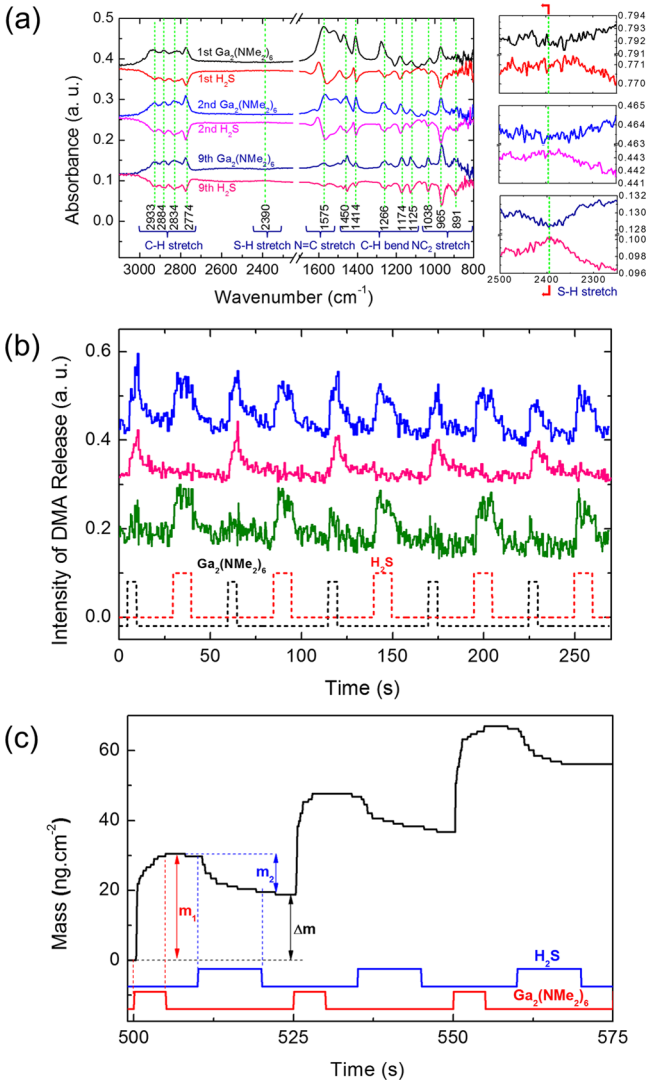

Figure 1. In situ measurements during Ga_2S_3 ALD using $Ga(N(CH_3)_2)_3$ and H_2S: (a) FTIR; (b) QMS; (c) QCM. Adapted from ref 15. Copyright 2014 American Chemical Society.

$N(CH_3)_2$ ligands retained on the surface after reaction 1. The blue trace in Figure 1b shows the QMS data for DMA collected during Ga_2S_3 ALD, whereas the red trace shows the "background" signal contributed by pulsing only the Ga compound. The green trace shows the difference, revealing that a majority of the DMA is released during the H_2S exposures. Quantitative analysis yielded $x = 0.3$, implying that only 10% of the $N(CH_3)_2$ ligands are released in reaction 1. Similarly, in situ quartz crystal microbalance (QCM) measurements disclosed the fraction of ligands remaining on the surface through the relative mass changes from each half-cycle. The relative mass loss (m_2/m_1) in Figure 1c implies $x = 0.35$, in excellent agreement with the QMS results. Unlike the FTIR and QMS measurements, QCM provides an unambiguous and quantitative measure of material growth. In particular, the net mass change of $\Delta m \approx 19$ ng/cm^2 per cycle in Figure 1c implies a GPC of 0.5 Å per cycle. It is noteworthy that fewer than one ligand (on average) is released during each Ga precursor exposure, suggesting that dissociative chemisorption is actually the dominant process in reaction 1, while the SH groups play a minor role.

The suite of in situ FTIR, QMS, and QCM is a powerful combination for elucidating the ALD mechanism, at least to the level of establishing the half-reactions. But ideally, one would know the location of each atom on the surface and in the gas phase at every instant during the ALD process. Scanning tunneling microscopy (STM) is an effective technique with sub-Ångstrom resolution for surface analysis. Recently, in situ STM was exploited during ZnS ALD to track the nucleation and growth of individual crystal grains after every cycle.[31] Quantum-mechanical calculations using density functional theory (DFT) are an excellent complement to ALD surface chemistry measurements for understanding thermodynamics, kinetics, and surface structures. For instance, DFT has been used to explain the decrease in CdS GPC with temperature[27] and also to elucidate the inhibition of PbS ALD on surfaces coated with self-assembled monolayers.[32]

One phenomenon that has emerged recently in ALD of mixed-metal sulfides is high cation mobility, leading to interdiffusion and even ion exchange. When ALD oxide films of different metals are deposited sequentially, the resulting composite typically maintains the as-deposited, nanolayered structure. In contrast, sulfide nanolaminates can rapidly intermix. For instance, a recent study of nanostructured thin films in the Zn−Sn−Cu sulfide system using secondary ion mass spectrometry depth profiling discovered that cation diffusion was rapid ($D = 3–5 \times 10^{-3}$ nm^2/s) in all cases with the exception of Sn in ZnS ($D < 8 \times 10^{-5}$ nm^2/s).[20] This rapid diffusion has also been shown to promote gas-phase ion exchange during the ALD of mixed-metal sulfide nanolayers. For example, exposing a 54 nm ZnS film to a single, prolonged exposure of bis(*N*,*N*′-di-*sec*-butylacetamidinato)dicopper(I) completely removed Zn from the film, presumably as volatile Zn amidinates, to produce a pure Cu_2S film.[33] These phenomena will complicate attempts to engineer precise ALD sulfide nanostructures. On the other hand, rapid intermixing can also facilitate the low-temperature synthesis of complex materials, as demonstrated for the quaternary sulfide Cu_2ZnSnS_4 (CZTS).[21]

■ ALD OF SULFIDES FOR PHOTOVOLTAICS

Solar energy conversion has a rich history in semiconducting thin films, a strong dependence on interfacial properties, and several technology families have been founded on chalcogenides. Therefore, the ALD of sulfides for photovoltaics (PVs) is a natural pairing. Most PVs have in common an absorber to harvest light, an emitter to form a rectifying junction, and often a buffer layer between the two to tune the charge transfer. ALD sulfides have been successfully implemented in each of these roles over the past decade and continue to drive our atomic-scale understanding of PV operation.

Absorbers

Compared with oxides, the band gaps and energy levels of chalcogenides are more suitable for harvesting solar energy. For single-absorber PVs, the maximum theoretical power efficiency is 31−34% for materials with band gaps in the range of 1.0 to 1.6 eV (Figure 2). The metal chalcogenides cover this band-gap range better than almost any other material class and further extend into the ideal range for tandem PVs (0.9 and 1.7 eV).

The semiconducting sulfides with band gaps suitable for solar energy conversion that have been synthesized by ALD are summarized in Table 1. The first solar absorber material to be successfully grown by ALD was $CuInS_2$.[43] This material

DOI: 10.1021/ar500360d
Acc. Chem. Res. 2015, 48, 341−348

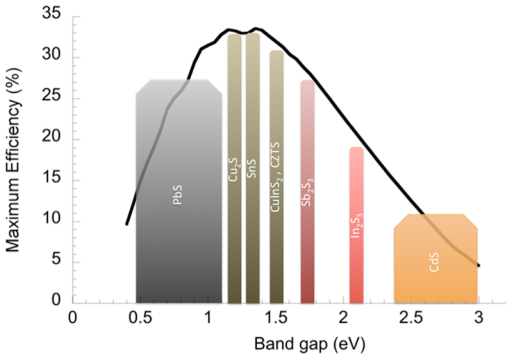

Figure 2. Single-junction efficiency limit, with band gaps of reported ALD sulfide processes highlighted.

Table 1. ALD Sulfide Solar Absorbers[a]

sulfide	band gap (eV)	majority carrier	type	power eff. (%)	record eff. (%)[34]	ref(s)
$CuInS_2$	1.5	p-type	ETA	4	12	35
CZTS	1.5	p-type	thin film	–	12.6	21
Cu_xS	1.2	p-type	ETA	<0.1	10	36
SnS	**1.3**	**p-type**	**thin film**	**4**	**4**	37, 38
PbS	0.4	p-type	QDSSC	0.6	6	39
Sb_2S_3	1.7	p-type	thin film	5.8	8	40
CdS	2.4	n-type	QDSSC	0.3	3	41
In_2S_3	2.1	n-type	ETA	0.4	3	42

[a]**Bold** denotes record power efficiency for any deposition method. ETA = extremely thin absorber. QDSSC = quantum-dot-sensitized solar cell.

belongs to a popular family of direct-gap, high-extinction absorbers with the chalcopyrite structure. Other members of the family, including $CuInSe_2$, $Cu(In,Ga)Se_2$, $Cu(In,Ga)(S,Se)_2$ (CIGS), and $Cu(Zn,Sn)(S,Se)_2$ (CZTS), now reach 21% power efficiency. Like many early ALD process, the original report[43] utilized high temperatures (>300 °C) and halide precursors. Although not completely self-limiting, careful alternation of CuCl and $InCl_3$ with H_2S gas produced a phase-pure $CuInS_2$ thin film. The conformal nature of ALD was leveraged to deposit $CuInS_2$ within a nanoporous TiO_2 framework, then phase-purified by annealing in H_2S.[44] Power efficiencies of up to 4% have been reported through this method, making these devices still some of the most efficient extremely thin absorber (ETA) cells and ALD-absorber PVs reported to date.[35]

The most complex ALD sulfide grown to date is quaternary CZTS.[21] This solar absorber is derived from the same CIGS family but replaces the rare and expensive In and Ga with earth-abundant Zn and Sn. While record efficiencies of CTZS PVs are currently limited to 12% (not by ALD), these earth-abundant cousins have the potential to scale to terawatt levels. In contrast to the halide-based and high-temperature ALD of $CuInS_2$, ALD of this quaternary composite was achieved at low temperatures (<150 °C) using metalorganic precursors. Even at these low temperatures, the system illustrates a primary difference from oxide ALD, that of cation displacement and interdiffusion during growth,[20,33,45] as described previously. Nevertheless, phase-pure and photoactive films were achieved after annealing under Ar for 2 h.

Cu_2S was one of the first thin-film PV technologies seriously explored, exhibiting power efficiencies hitting the 10% milestone in 1980, before either CdTe or CIGS. However, a stoichiometric, CdS-free, and *stable* Cu_2S p–n junction has been elusive via physical vapor deposition, Cu metal sulfurization, CVD, and solution methods. In contrast, the low temperature and chemically tunable properties of ALD allow highly stoichiometric, desirably doped (10^{17} cm^{-3}), and oriented crystalline thin films.[46,47] Furthermore, with ALD-grown oxide overlayers, the electronic properties of these films have been stabilized against the oxidative effects of ambient exposure for at least 1 month.[47,48]

Although a stable Cu_2S PV device has yet to be demonstrated, ALD of p-type SnS has produced record efficiencies. Tin(II) acetylacetonate or N^2,N^3-di-*tert*-butylbutane-2,3-diamidotin(II) alternation with H_2S produces clean and lightly doped (10^{15} cm^{-3}) thin films with high mobilities (up to 10 cm^2 V^{-1} s^{-1}) that enable external quantum efficiencies of over 90%.[14,17,29] The co-optimization of SnS electronic properties alongside ALD-grown Zn(O,S) allowed for a record device efficiency of 4%.[37]

Quantum-dot-sensitized solar cells (QDSSCs) are a third class of PV that have benefited from sulfide ALD. As alternatives to the molecular dyes found in prototypical dye-sensitized solar cells (DSSCs), PbS[39] and CdS[41] have been used to sensitize porous TiO_2. ALD is uniquely suited to uniformly coat these high-surface-area frameworks as well as to fine-tune the QD size, and therefore the energy levels, simply with the number of cycles.

Emitters and Buffer Layers

While a lightly doped absorber can minimize recombination where photogenerated carriers are produced, a more heavily doped wide-band-gap material (emitter or window layer) is preferred to minimize parasitic absorption and maximize the charge-separating electric field. Additionally, an ultrathin buffer layer may be inserted between the absorber and emitter to minimize performance-stealing defects. Several common sulfide emitters and buffer layers, including In_2S_3, ZnS, and CdS, and oxysulfides (e.g. Zn(O,S)), have been grown by ALD for PV. The conformal and ultrathin nature of the ALD layers minimizes dead zones and parasitic light absorption, respectively. A second advantage is the ease of achieving tunable or even graded compositions by ALD. In this way, the energy level mismatch can be tuned to avoid a barrier to charge transfer across the p–n junction.[38] ALD-based buffer layers for interfacial engineering have been reviewed previously.[49]

■ ALD OF SULFIDES FOR ENERGY STORAGE

Electrical energy storage (EES) devices are essential for the implementation of renewable energy resources for portable electronics, transportation, and smart grids. Among the various EES technologies, batteries are the most widely used, and lithium-ion batteries (LIBs) currently dominate consumer electronics. To enable the utilization of LIBs in transportation and grid-level storage, several challenges remain in cost, safety, and energy density. LIB performance is ultimately determined by materials, and extensive efforts to develop improved materials are underway. Sulfides are particularly promising for EES, and they can be used in lithium-based batteries as anodes, cathodes, and/or solid-state electrolytes.

ALD has been used in two main technical routes to address these challenges:[50] (1) rational design of nanostructured materials as electrodes and solid-state electrolytes and (2) atomic-scale surface coatings for interfacial modifications

DOI: 10.1021/ar500360d
Acc. Chem. Res. 2015, 48, 341–348

between electrodes and liquid electrolytes. Among the sulfide materials deposited by ALD, only limited species to date have been investigated for battery applications, including GaS_x, Cu_2S, and Li_2S. ALD is both an elegant technique for atomically controlled deposition of nanoscale films for microbatteries and a viable route for mass production of nanostructured materials for bulk-type batteries. The former is critical in autonomous systems (e.g., hearing aids and medical implants) while the latter is essential for electric vehicles and smart grids. ALD can provide both high energy density and reliable charge−discharge cycling.

Meng and co-workers developed nanoscale ALD GaS_x films for microbatteries[15] and core−shell nanocomposites (Figure 3)

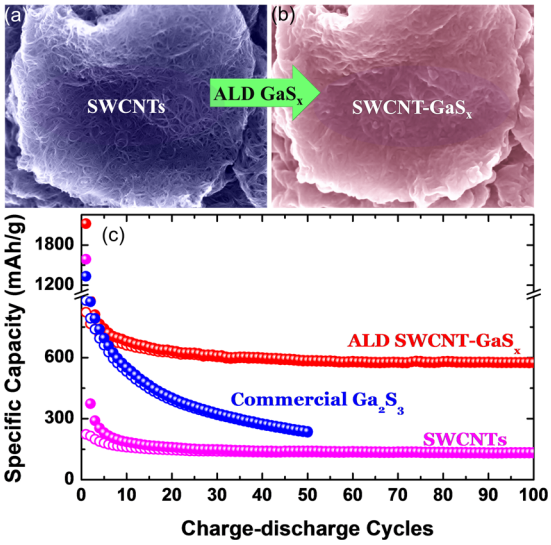

Figure 3. (a, b) SEM images of (a) commercial SWCNTs and (b) ALD GaS_x-coated SWCNTs. (c) Cyclability and capacity of commercial Ga_2S_3, SWCNTs, and ALD SWCNT-GaS_x.[16] Adapted with permission from ref 16. Copyright 2014 Wiley-VCH.

of GaS_x supported by networked single-walled carbon nanotubes (SWCNTs) for bulk-type batteries.[16] ALD GaS_x anodes performed much better than microsized Ga_2S_3 in sustainable capacity, cyclability, and rate capability, accounting for a capacity of >700 mA h g^{-1} for 100 cycles. This is twice the theoretical capacity of graphite (372 mA h g^{-1}), which dominates commercial LIBs. In comparison with anodes, effort on new cathodes is even more significant, as the traditional lithium metal oxides (e.g., $LiCoO_2$ and $LiMn_2O_4$) have capacities below 200 mA h g^{-1}. Recent work reported core−shell-nanostructured SWCNT−Cu_2S composites via ALD that achieve a capacity of ∼260 mA h g^{-1} for 200 cycles.[51] Another recent work examined ALD Li_2S as a cathode.[19] As a lithium-containing cathode material, Li_2S has a maximum capacity of 1166 mA h g^{-1}. From LiO^{t}Bu and H_2S as precursors, ALD Li_2S demonstrated high stability, a sustainable capacity of ∼800 mA h g^{-1}, and high rate capability in Li−S batteries. Li−S batteries hold great promise for electric vehicles, since they promise an energy density 5 times greater than that of LIBs and significantly reduced cost.[52]

■ ALD OF SULFIDES FOR PHOTONICS

ALD of sulfide materials such as ZnS:Mn was first developed to manufacture TFEL displays. As described earlier, a variety of precursors exist for ZnS:Mn ALD, and precursor selection is critical to the aging behavior of these films since it controls impurities and defects in both the film and microstructure.[22] Despite these challenges, ALD-enabled TFEL displays represent the first commercial success for ALD sulfides and are now manufactured at large scale by Lumineq.

ALD ZnS has also been explored for other photonic applications. For example, by the combination of ALD ZnS and Al_2O_3 as model high- and low-refractive-index materials, antireflective coatings, Fabry−Perot filters, and neutral beamsplitters were fabricated.[53] Multilayer stacks can be fabricated with precise control of the layer thicknesses, demonstrating an advantage of ALD for optical materials. However, roughness induced by the polycrystalline ZnS films complicates the formation of atomically flat interfaces.

ALD can also be used to fabricate three-dimensional (3D) photonic crystals. To demonstrate this concept, ZnS:Mn films were deposited conformally within self-assembled silica nanosphere arrays, filling >95% of the pore volume.[54] These structures exhibited strong photoluminescence, showing the potential of this technique to create high-quality nanophotonic structures. This process was extended to the fabrication of multilayer coatings of ZnS:Mn and TiO_2 for inverse opal geometries (Figure 4a), further tuning their photoluminescence.[55] These structures combine several advantages of ALD, including conformality, thickness control, precise doping, and

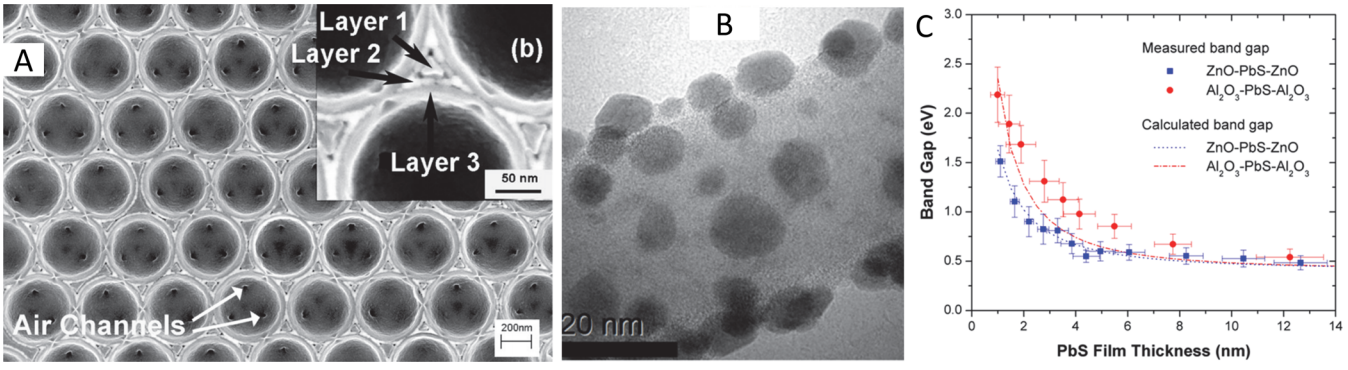

Figure 4. Sulfide photonic structures. (a) SEM image of a TiO_2/ZnS:Mn multilayer photonic crystal. Reproduced with permission from ref 55. Copyright 2006 American Institute of Physics. (b) TEM image of PbS QDs deposited on a Si nanowire surface. Reproduced from ref 57. Copyright 2011 American Chemical Society. (c) Band-gap variation in ALD PbS films by thickness control. Reproduced with permission from ref 58. Copyright 2010 IOP Publishing.

DOI: 10.1021/ar500360d
Acc. Chem. Res. 2015, 48, 341−348

nanolaminate growth, into a single material with tunable properties.

Another interesting class of photonic materials is quantum-confinement structures. These materials exhibit tunable optical and electronic properties when one or more of their dimensions are reduced to below their Bohr exciton radii. Metal chalcogenide materials have been widely studied as quantum-confinement structures because of their favorable material properties. For example, PbS is a direct-gap semiconductor with a bulk band gap of ∼0.4 eV and a Bohr exciton radius of ∼18 nm, making it interesting for quantum-confinement studies.

To test the ability of ALD to tune the properties of PbS, thin films and isolated nanoparticles were fabricated and evaluated.[56,57] The nucleation of PbS on SiO_2 surfaces follows an island growth mechanism, resulting in the direct formation of quantum dots during the initial ALD cycles.[57] These islands eventually coalesce into polycrystalline films, which act as quantum wells until they are sufficiently thick. Their band gaps have been measured by a variety of techniques[56−59] and can be tuned across a wide range of visible and near-IR wavelengths by control of the number of ALD cycles (Figure 4c). Because of the dispersion in particle diameter, which increases with cycle number, a broad photoluminescence spectrum is observed,[57] and a distribution of band gaps were recorded in localized measurements. The band gap can also be adjusted by the choice of the barrier material surrounding the PbS,[58] illustrating the power of ALD for band-gap engineering.

The size and shape of the PbS QDs can be further modified by ex situ or in situ annealing, which leads to a decrease in the average and standard deviation of the QD diameter as well as an evolution to dome-shaped particles.[57,60] This ability to create isolated, dome-shaped QDs was used to probe localized variations in the electronic structure *within* individual pristine QDs using electron energy loss spectroscopy (EELS).[59] The localized electronic structure was seen to vary with position within the QD as a result of the anisotropic shape. This demonstrates the power of ALD to control of size and shape in quantum-confined particles without the need for surfactants or strain-induced epitaxial growth methods.

To demonstrate the power of ALD for hierarchical nanostructure growth, PbS QDs were conformally deposited directly onto nanowire surfaces (Figure 4b)[57] with sizes dictated by the number of ALD cycles. These conformal 3D structures would be very difficult to synthesize by other techniques, suggesting the possibility of fabricating unique devices such as QD-sensitized nanowire PVs or photodetectors, which would take advantage of both the photonic properties of the nanowire template and the tunable band gap of the QD structures.

■ CONCLUSIONS AND FUTURE OUTLOOK

ALD was invented when ZnS was deposited nearly 40 years ago. Despite this pedigree, metal sulfides have remained relatively unexplored. However, increasing performance demands in applications such as photovoltaics, energy storage, and nanophotonics, coupled with the chemical and structural advantages of ALD, have rekindled interest in sulfides. Progress is likely to be rapid given the wealth of knowledge and experience amassed in the development of oxides, and sulfide processes covering most of the technologically relevant metals will surely emerge. Nevertheless, challenges unique to sulfides such as ion exchange, air reactivity, and H_2S toxicity require attention if these new processes are to be incorporated into device manufacturing. Finally, the recent focus on 2D layered materials will likely seed interest in chalcogenide ALD.

■ AUTHOR INFORMATION

Corresponding Authors

*E-mail: ndasgupt@umich.edu.
*E-mail: jelam@anl.gov.
*E-mail: martinson@anl.gov.

Author Contributions

[‖]N.P.D. and X.M. contributed equally.

Notes

The authors declare no competing financial interest.

Biographies

Neil P. Dasgupta is an Assistant Professor of Mechanical Engineering at the University of Michigan. He earned his Ph.D. in Mechanical Engineering from Stanford University in 2011 and was a Postdoctoral Fellow in the Department of Chemistry at University of California, Berkeley in 2012−2013. His current research focuses on the application of ALD, semiconductor nanowires, and hierarchical nanomaterials for energy and sustainability applications.

Xiangbo Meng is a Postdoctoral Fellow at Argonne National Laboratory in Argonne, Illinois. He earned a Ph.D. in Mechanical and Materials Engineering in 2011 and another Ph.D. in Chemical and Biochemical Engineering in 2008 at The University of Western Ontario, Canada. He was awarded an NSERC Postdoctoral Fellowship from 2011 to 2013 and worked as a Postdoctoral Fellow at Brookhaven National Laboratory in 2011−2012. His current research focuses on the development of nanostructured materials and next-generation battery systems.

Jeffrey W. Elam is a Principal Chemist and Group Leader at Argonne National Laboratory. He received his Ph.D. in Physical Chemistry from the University of Chicago and was a Postdoctoral Fellow with Steven M. George at the University of Colorado, Boulder. His interests range from ALD chemistry and materials to the scale-up and commercialization of ALD technology.

Alex B. F. Martinson is a Chemist and Principal Investigator in the Surface Chemistry Group at Argonne National Laboratory. He earned his Ph.D. in Physical Chemistry from Northwestern University and was a Director's Postdoctoral Fellow in the Materials Science Division at Argonne National Laboratory. His interests involve novel control of interfaces and materials for energy applications, including solar electricity, fuels, and chemical energy conversion.

■ ACKNOWLEDGMENTS

Work by J.W.E. and X.M. was supported as part of the Center for Electrical Energy Storage: Tailored Interfaces, an Energy Frontier Research Center funded by the U.S. Department of Energy, Office of Science, Office of Basic Energy Sciences. Work at ANL was supported under U.S. DOE Contract DE-AC02-06CH11357. N.P.D. acknowledges support from the Joint Center for Energy Storage Research (JCESR), an Energy Innovation Hub funded by the U.S. Department of Energy, Office of Science, Basic Energy Sciences. Work by A.B.F.M. was supported as part of the Argonne-Northwestern Solar Energy Research (ANSER) Center, an Energy Frontier Research Center funded by the U.S. Department of Energy (DOE), Office of Science, Basic Energy Sciences (BES), under Award # DE-SC0001059.

DOI: 10.1021/ar500360d
Acc. Chem. Res. 2015, 48, 341−348

REFERENCES

(1) George, S. M. Atomic Layer Deposition: An Overview. *Chem. Rev.* **2010**, *110*, 111−131.
(2) Suntola, T.; Hyvarinen, J. Atomic Layer Epitaxy. *Annu. Rev. Mater. Sci.* **1985**, *15*, 177−195.
(3) Dasgupta, N. P.; Mack, J. F.; Langston, M. C.; Bousetta, A.; Prinz, F. B. Design of an atomic layer deposition reactor for hydrogen sulfide compatibility. *Rev. Sci. Instrum.* **2010**, *81*, No. 044102.
(4) Suntola, T. Atomic layer epitaxy. *Mater. Sci. Rep.* **1989**, *4*, 261−312.
(5) Suntola, T.; Antson, J. Method for producing compound thin films. U.S. Patent 4,058,430, 1977.
(6) Tammenmaa, M.; Antson, H.; Asplund, M.; Hiltunen, L.; Leskelä, M.; Niinistö, L.; Ristolainen, E. Alkaline-Earth Sulfide Thin Films Grown by Atomic Layer Epitaxy. *J. Cryst. Growth* **1987**, *84*, 151−154.
(7) Stanley, A. E. Synthesis of cadmium sulfide using the spontaneous reaction of dialkylcadmium and hydrogen sulfide. U.S. Patent H000459, 1988.
(8) Leskelä, M.; Niinistö, L.; Niemela, P.; Nykänen, E.; Soininen, P.; Tiitta, M.; Vähäkangas, J. Preparation of Lead Sulfide Thin Films by the Atomic Layer Epitaxy Process. *Vacuum* **1990**, *41*, 1457−1459.
(9) Asikainen, T.; Ritala, M.; Leskelä, M. Growth of In_2S_3 Thin-Films by Atomic Layer Epitaxy. *Appl. Surf. Sci.* **1994**, *82*−*3*, 122−125.
(10) Meester, B.; Reijnen, L.; Goossens, A.; Schoonman, J. Comparative study of atomic layer deposition and low-pressure MOCVD of copper sulfide thin films. *J. Phys. IV* **2001**, *11*, 1147−1152.
(11) Scharf, T. W.; Prasad, S. V.; Mayer, T. M.; Goeke, R. S.; Dugger, M. T. Atomic layer deposition of tungsten disulphide solid lubricant thin films. *J. Mater. Res.* **2004**, *19*, 3443−3446.
(12) Pore, V.; Ritala, M.; Leskelä, M. Atomic layer deposition of titanium disulfide thin films. *Chem. Vap. Deposition* **2007**, *13*, 163−168.
(13) Yang, R. B.; Bachmann, J.; Reiche, M.; Gerlach, J. W.; Gosele, U.; Nielsch, K. Atomic Layer Deposition of Antimony Oxide and Antimony Sulfide. *Chem. Mater.* **2009**, *21*, 2586−2588.
(14) Kim, J. Y.; George, S. M. Tin Monosulfide Thin Films Grown by Atomic Layer Deposition Using Tin 2,4-Pentanedionate and Hydrogen Sulfide. *J. Phys. Chem. C* **2010**, *114*, 17597−17603.
(15) Meng, X.; Libera, J. A.; Fister, T. T.; Zhou, H.; Hedlund, J. K.; Fenter, P.; Elam, J. W. Atomic Layer Deposition of Gallium Sulfide Films Using Hexakis(dimethylamido)digallium and Hydrogen Sulfide. *Chem. Mater.* **2014**, *26*, 1029−1039.
(16) Meng, X.; He, K.; Su, D.; Zhang, X.; Sun, C.; Ren, Y.; Wang, H.-H.; Weng, W.; Trahey, L.; Canlas, C. P.; Elam, J. W. Gallium Sulfide−Single-Walled Carbon Nanotube Composites: High-Performance Anodes for Lithium-Ion Batteries. *Adv. Funct. Mater.* **2014**, *24*, 5435−5442.
(17) Kim, S. B.; Sinsermsuksakul, P.; Hock, A. S.; Pike, R. D.; Gordon, R. G. Synthesis of N-Heterocyclic Stannylene (Sn(II)) and Germylene (Ge(II)) and a Sn(II) Amidinate and Their Application as Precursors for Atomic Layer Deposition. *Chem. Mater.* **2014**, *26*, 3065−3073.
(18) Tan, L. K.; Liu, B.; Teng, J. H.; Guo, S.; Low, H. Y.; Loh, K. P. Atomic layer deposition of a MoS_2 film. *Nanoscale* **2014**, *6*, 10584−10588.
(19) Meng, X.; Comstock, D. J.; Fister, T. T.; Elam, J. W. Vapor-phase atomic-controllable growth of amorphous Li_2S for high-performance lithium−sulfur batteries. *ACS Nano* **2014**, *8*, 10963−10972.
(20) Thimsen, E.; Baryshev, S. V.; Martinson, A. B. F.; Elam, J. W.; Veryovkin, I. V.; Pellin, M. J. Interfaces and Composition Profiles in Metal−Sulfide Nanolayers Synthesized by Atomic Layer Deposition. *Chem. Mater.* **2013**, *25*, 313−319.
(21) Thimsen, E.; Riha, S. C.; Baryshev, S. V.; Martinson, A. B. F.; Elam, J. W.; Pellin, M. J. Atomic Layer Deposition of the Quaternary Chalcogenide Cu_2ZnSnS_4. *Chem. Mater.* **2012**, *24*, 3188−3196.
(22) Ihanus, J.; Lankinen, M. P.; Kemell, M.; Ritala, M.; Leskelä, M. Aging of electroluminescent ZnS:Mn thin films deposited by atomic layer deposition processes. *J. Appl. Phys.* **2005**, *98*, No. 113526.
(23) Puurunen, R. L. Surface chemistry of atomic layer deposition: A case study for the trimethylaluminum/water process. *J. Appl. Phys.* **2005**, *97*, No. 121301.
(24) Miikkulainen, V.; Leskelä, M.; Ritala, M.; Puurunen, R. L. Crystallinity of inorganic films grown by atomic layer deposition: Overview and general trends. *J. Appl. Phys.* **2013**, *113*, No. 021301.
(25) Bakke, J. R.; King, J. S.; Jung, H. J.; Sinclair, R.; Bent, S. F. Atomic layer deposition of ZnS via in situ production of H_2S. *Thin Solid Films* **2010**, *518*, 5400−5408.
(26) Tanskanen, J. T.; Bakke, J. R.; Pakkanen, T. A.; Bent, S. F. Influence of organozinc ligand design on growth and material properties of ZnS and ZnO deposited by atomic layer deposition. *J. Vac. Sci. Technol., A* **2011**, *29*, No. 031507.
(27) Bakke, J. R.; Jung, H. J.; Tanskanen, J. T.; Sinclair, R.; Bent, S. F. Atomic Layer Deposition of CdS Films. *Chem. Mater.* **2010**, *22*, 4669−4678.
(28) Saanila, V.; Ihanus, J.; Ritala, M.; Leskelä, M. Atomic layer epitaxy growth of BaS and BaS:Ce thin films from in situ synthesized $Ba(thd)_2$. *Chem. Vap. Deposition* **1998**, *4*, 227−233.
(29) Sinsermsuksakul, P.; Heo, J.; Noh, W.; Hock, A. S.; Gordon, R. G. Atomic Layer Deposition of Tin Monosulfide Thin Films. *Adv. Energy Mater.* **2011**, *1*, 1116−1125.
(30) Ham, G.; Shin, S.; Park, J.; Choi, H.; Kim, J.; Lee, Y. A.; Seo, H.; Jeon, H. Tuning the Electronic Structure of Tin Sulfides Grown by Atomic Layer Deposition. *ACS Appl. Mater. Interfaces* **2013**, *5*, 8889−8896.
(31) Mack, J. F.; Van Stockum, P. B.; Yemane, Y. T.; Logar, M.; Iwadate, H.; Prinz, F. B. Observing the Nucleation Phase of Atomic Layer Deposition in Situ. *Chem. Mater.* **2012**, *24*, 4357−4362.
(32) Lee, W.; Dasgupta, N. P.; Trejo, O.; Lee, J. R.; Hwang, J.; Usui, T.; Prinz, F. B. Area-Selective Atomic Layer Deposition of Lead Sulfide: Nanoscale Patterning and DFT Simulations. *Langmuir* **2010**, *26*, 6845−6852.
(33) Thimsen, E.; Peng, Q.; Martinson, A. B. F.; Pellin, M. J.; Elam, J. W. Ion Exchange in Ultrathin Films of Cu_2S and ZnS under Atomic Layer Deposition Conditions. *Chem. Mater.* **2011**, *23*, 4411−4413.
(34) Green, M. A.; Emery, K.; Hishikawa, Y.; Warta, W.; Dunlop, E. D. Solar cell efficiency tables (version 44). *Prog. Photovoltaics* **2014**, *22*, 701−710.
(35) Nanu, M.; Schoonman, J.; Goossens, A. Solar-energy conversion in $TiO_2/CuInS_2$ nanocomposites. *Adv. Funct. Mater.* **2005**, *15*, 95−100.
(36) Reijnen, L.; Meester, B.; Goossens, A.; Schoonman, J. Atomic layer deposition of Cu_xS for solar energy conversion. *Chem. Vap. Deposition* **2003**, *9*, 15−20.
(37) Sinsermsuksakul, P.; Sun, L.; Lee, S. W.; Park, H. H.; Kim, S. B.; Yang, C.; Gordon, R. G. Overcoming Efficiency Limitations of SnS-Based Solar Cells. *Adv. Energy Mater.* **2014**, *4*, No. 1400496.
(38) Sinsermsuksakul, P.; Hartman, K.; Kim, S. B.; Heo, J.; Sun, L. Z.; Park, H. H.; Chakraborty, R.; Buonassisi, T.; Gordon, R. G. Enhancing the efficiency of SnS solar cells via band-offset engineering with a zinc oxysulfide buffer layer. *Appl. Phys. Lett.* **2013**, *102*, No. 053901.
(39) Brennan, T. P.; Trejo, O.; Roelofs, K. E.; Xu, J.; Prinz, F. B.; Bent, S. F. Efficiency enhancement of solid-state PbS quantum dot-sensitized solar cells with Al_2O_3 barrier layer. *J. Mater. Chem. A* **2013**, *1*, 7566−7571.
(40) Kim, D.-H.; Lee, S.-J.; Park, M. S.; Kang, J.-K.; Heo, J.-H.; Im, S. H.; Sung, S.-J. Highly reproducible planar Sb_2S_3-sensitized solar cells based on atomic layer deposition. *Nanoscale* **2014**, *6*, 14549−14554.
(41) Brennan, T. P.; Ardalan, P.; Lee, H. B. R.; Bakke, J. R.; Ding, I. K.; McGehee, M. D.; Bent, S. F. Atomic Layer Deposition of CdS Quantum Dots for Solid-State Quantum Dot Sensitized Solar Cells. *Adv. Energy Mater.* **2011**, *1*, 1169−1175.
(42) Sarkar, S. K.; Kim, J. Y.; Goldstein, D. N.; Neale, N. R.; Zhu, K.; Elliot, C. M.; Frank, A. J.; George, S. M. In_2S_3 Atomic Layer Deposition and Its Application as a Sensitizer on TiO_2 Nanotube Arrays for Solar Energy Conversion. *J. Phys. Chem. C* **2010**, *114*, 8032−8039.

DOI: 10.1021/ar500360d
Acc. Chem. Res. 2015, 48, 341−348

(43) Nanu, M.; Reijnen, L.; Meester, B.; Schoonman, J.; Goossens, A. $CuInS_2$ thin films deposited by ALD. *Chem. Vap. Deposition* **2004**, *10*, 45−49.
(44) Nanu, M.; Schoonman, J.; Goossens, A. Inorganic nanocomposites of n- and p-type semiconductors: A new type of three-dimensional solar cell. *Adv. Mater.* **2004**, *16*, 453−456.
(45) Genevee, P.; Donsanti, F.; Schneider, N.; Lincot, D. Atomic layer deposition of zinc indium sulfide films: Mechanistic studies and evidence of surface exchange reactions and diffusion processes. *J. Vac. Sci. Technol., A* **2013**, *31*, No. 01A131.
(46) Martinson, A. B. F.; Elam, J. W.; Pellin, M. J. Atomic layer deposition of Cu_2S for future application in photovoltaics. *Appl. Phys. Lett.* **2009**, *94*, No. 123107.
(47) Martinson, A. B. F.; Riha, S. C.; Thimsen, E.; Elam, J. W.; Pellin, M. J. Structural, optical, and electronic stability of copper sulfide thin films grown by atomic layer deposition. *Energy Environ. Sci.* **2013**, *6*, 1868−1878.
(48) Riha, S. C.; Jin, S.; Baryshev, S. V.; Thimsen, E.; Wiederrecht, G. P.; Martinson, A. B. F. Stabilizing Cu_2S for Photovoltaics One Atomic Layer at a Time. *ACS Appl. Mater. Interfaces* **2013**, *5*, 10302−10309.
(49) Bakke, J. R.; Pickrahn, K. L.; Brennan, T. P.; Bent, S. F. Nanoengineering and interfacial engineering of photovoltaics by atomic layer deposition. *Nanoscale* **2011**, *3*, 3482−3508.
(50) Meng, X. B.; Yang, X. Q.; Sun, X. L. Emerging Applications of Atomic Layer Deposition for Lithium-Ion Battery Studies. *Adv. Mater.* **2012**, *24*, 3589−3615.
(51) Meng, X.; Riha, S.; Fister, T.; Trahey, L.; Martinson, A.; Fenter, P.; Elam, J. W. Atomic Layer Deposited Cu_2S as a Superior Electrode Material with High Capacity and Excellent Cycleability for Lithium-Ion Batteries. *ECS Meet. Abstr.* **2013**, *MA2013−02*, 1028.
(52) Ji, X.; Lee, K. T.; Nazar, L. F. A highly ordered nanostructured carbon−sulphur cathode for lithium−sulphur batteries. *Nat. Mater.* **2009**, *8*, 500−506.
(53) Riihelä, D.; Ritala, M.; Matero, R.; Leskelä, M. Introducing atomic layer epitaxy for the deposition of optical thin films. *Thin Solid Films* **1996**, *289*, 250−255.
(54) King, J. S.; Neff, C. W.; Summers, C. J.; Park, W.; Blomquist, S.; Forsythe, E.; Morton, D. High-filling-fraction inverted ZnS opals fabricated by atomic layer deposition. *Appl. Phys. Lett.* **2003**, *83*, 2566−2568.
(55) King, J. S.; Graugnard, E.; Summers, C. J. Photoluminescence modification by high-order photonic bands in TiO_2/ZnS:Mn multilayer inverse opals. *Appl. Phys. Lett.* **2006**, *88*, No. 081109.
(56) Dasgupta, N. P.; Lee, W.; Prinz, F. B. Atomic Layer Deposition of Lead Sulfide Thin Films for Quantum Confinement. *Chem. Mater.* **2009**, *21*, 3973−3978.
(57) Dasgupta, N. P.; Jung, H. J.; Trejo, O.; McDowell, M. T.; Hryciw, A.; Brongersma, M.; Sinclair, R.; Prinz, F. B. Atomic Layer Deposition of Lead Sulfide Quantum Dots on Nanowire Surfaces. *Nano Lett.* **2011**, *11*, 934−940.
(58) Lee, W.; Dasgupta, N. P.; Jung, H. J.; Lee, J. R.; Sinclair, R.; Prinz, F. B. Scanning tunneling spectroscopy of lead sulfide quantum wells fabricated by atomic layer deposition. *Nanotechnology* **2010**, *21*, No. 485402.
(59) Jung, H. J.; Dasgupta, N. P.; Van Stockum, P. B.; Koh, A. L.; Sinclair, R.; Prinz, F. B. Spatial Variation of Available Electronic Excitations within Individual Quantum Dots. *Nano Lett.* **2013**, *13*, 716−721.
(60) Langston, M. C.; Dasgupta, N. P.; Jung, H. J.; Logar, M.; Huang, Y.; Sinclair, R.; Prinz, F. B. In Situ Cycle-by-Cycle Flash Annealing of Atomic Layer Deposited Materials. *J. Phys. Chem. C* **2012**, *116*, 24177−24183.

DOI: 10.1021/ar500360d
Acc. Chem. Res. 2015, 48, 341−348